

Constellation Labeling for Linear Encoders

Richard D. Wesel, *Senior Member, IEEE*, Xueting Liu, *Member, IEEE*, John M. Cioffi, *Fellow, IEEE*, and Christos Kominakis, *Student Member, IEEE*

Abstract—This paper investigates optimal constellation labeling in the context of the edge profile. A constellation's edge profile lists the minimum-distance edge for each binary symbol error. The paper introduces the symmetric-ultracomposite (SU) labeling structure and shows that this structure provides undominated edge profiles for 2^n -PSK, 2^n -PAM, and 2^{2n} -point square QAM. The SU structure is a generalization of the commonly used reflected binary Gray code. With the proper choice of basis vectors, SU labeling can support either set-partition or Gray-code labeling of 2^n -PSK, 2^n -PAM, and 2^{2n} -point square QAM. Notably, there are Gray-code and set-partition labelings that do not have the SU structure. These labelings yield inferior edge profiles.

The SU structure does not apply to cross constellations. However, for any standard cross constellation with 32 or more points, a quasi-SU labeling structure can approximate the SU structure. With the correct choice of basis, quasi-SU labelings produce quasi-Gray labelings. However, the quasi-SU structure cannot support set-partition labeling. In fact, the quasi-SU structure provides a better edge profile than standard set-partition labeling. Thus, for cross constellations there is a choice between edge profile optimality and the group structure provided by set-partitioning. Here, the correct choice depends on whether the encoder trellis has parallel branches.

Index Terms—Binary reflected labeling, coded modulation, constellation labeling, fading channels, Gray code, set-partition.

I. INTRODUCTION

MANY searches for trellis codes pick a single constellation labeling and search over a set of convolutional codes. While the choice of convolutional code is the result of an exhaustive search, the choice of labeling is often not justified beyond stating that the labeling is a Gray-code (GC) labeling [1] or a set-partitioning (SP) labeling [2], [3].

A GC-labeled constellation is one where any two points that are nearest neighbors have binary labels that differ in exactly one bit position. The SP labeling paradigm partitions the constellation into a collection of mutually exclusive, collectively exhaustive subsets (called cosets because of their algebraic structure) so as to maximize the separation between nearest neighbors in

the same coset. Following the approach set forth in [2], coset membership is identified by the least significant bits (LSBs) of the point labels.

There is conventional wisdom that among the many possible permutations of SP and GC labelings, the particular choice does not matter much as long as it is sensible. However, there is no precise notion of what is meant by sensible, and such conventional wisdom is passed among a relatively small group of code designers. It is not readily available in the literature.

We imagine that the mathematically inclined designer, either unaware of the conventional wisdom or unsatisfied with it, may be distracted by considering various permutations of SP or GC labelings. Such a designer might notice, for example, that there are structurally distinct labelings that meet the SP paradigm and wonder which is best. Indeed, when SP is presented in our coding courses, a recurring question is whether it makes any difference which branches in the partition tree are labeled with a one and which with a zero.

The purpose of this paper is to formally answer the fundamental questions surrounding the selection of a constellation labeling for a standard trellis-coded modulation (TCM) without resorting to brute-force combinatorics. Our analysis must restrict attention to linear convolutional encoders. Consideration of general nonlinear encoders nullifies the role of constellation labeling. Such encoders permit a nonlinear table lookup just before the signal mapper that effectively relabels the constellation.

Consistent with the conventional wisdom, the difference in performance is small between the labelings we identify as desirable and slight permutations that are inferior. However, we do not seek out the very worst labelings (those that are not "sensible") since such labelings would serve no purpose but to make the best labelings seem even better in contrast.

For pulse-amplitude modulation (PAM), phase-shift keying (PSK), and 2^{2n} -QAM (square) constellations, it turns out that a single labeling structure (which we will call symmetric ultracomposite when we define it in Section III) stands out as a clear choice. This single structure supports both GC and SP labeling through appropriate choices of basis. For the cross constellations with 32 or more points, there is a choice between two distinct structures: SP labeling and an approximation of the symmetric-ultracomposite structure. The best choice depends on the application.

Section II examines constellation labeling in terms of the TCMS possible with a given labeling. One indication of the quality of a labeling for TCM is a list of distances we call the constellation's edge profile. For each binary symbol error, the **edge profile** includes the minimum Euclidean distance separating two points whose binary point-label difference is that binary symbol error. Section II also demonstrates that there are

Manuscript received December 20, 1998; revised March 9, 2001. This work was supported by the National Science Foundation under CAREER Award CCR-9733089, SBC Technology Resources, Inc., through California MICRO Program Project 98-169, and the Xetron Corporation. The material in this paper were presented in part at IEEE GLOBECOM 97, Phoenix, AZ, November 3–8, 1997, the 36th Annual Allerton Conference, Monticello, IL, September 23–25, 1998, and ICC-2000, New Orleans, LA, June 18–22, 2000.

R. D. Wesel, X. Liu, and C. Kominakis are with the Electrical Engineering Department, University of California at Los Angeles, Los Angeles, CA 90095-1594 USA (e-mail: wesel@ee.ucla.edu; xueting@ee.ucla.edu; chkomm@ee.ucla.edu).

J. M. Cioffi is with the Electrical Engineering Department, Stanford University, Stanford, CA 94305-9510 USA (e-mail: cioffi@stanford.edu).

Communicated by T. E. Fuja, Associate Editor At Large.

Publisher Item Identifier S 0018-9448(01)06223-X.

distinct structures within the standard paradigms of GC and SP labeling by showing that some labelings have a more desirable edge profile than other labelings within the specified paradigm.

Section III introduces symmetric-ultracomposite (SU) labeling, which is a generalization of the common binary reflected GC labeling. This section proves that for standard PAM, PSK, and 2^{2n} -QAM constellations, no labeling can provide an edge profile strictly better than the one provided by SU labeling. The SU structure may be used in either the GC or the SP paradigm, in both cases producing labelings already in common use.

Section IV proves that 2^{2n+1} cross constellations must have at least $2n+2$ minimum-distance edges, which implies that they cannot be GC labeled. This section then presents a procedure to convert a $2^n \times 2^{n+1}$ rectangular constellation with SU labeling into a labeled 2^{2n+1} cross constellation with exactly $2n+2$ minimum-distance edges. We call this cross-labeling structure quasi-SU.

With the correct choice of basis, quasi-SU labelings produce a quasi-Gray labeling. However, the quasi-SU structure cannot support SP labeling. In fact, the standard SP labelings of cross constellations with 32 or more points have at least $2n+4$ minimum-distance edges. Thus, for cross constellations there is a choice between the group structure provided by SP and the desirable edge profile provided by quasi-SU. Low-complexity code searches indicate that the superior edge profile is preferable when the best encoder trellis has no parallel branches. When the best encoder has parallel trellis branches, the group structure provided by SP produces a larger free Euclidean distance.

Section V concludes the paper.

II. CONSTELLATION LABELING AND TRELLIS CODES

This section examines constellation labeling in terms of the TCMs achievable for a given labeling. Section II-A introduces the worst-case mapping and the edge profile as quantitative indications of a constellation's labeling structure. Section II-B discusses the close relationship between the worst-case mapping and the free Euclidean distance of a trellis code. Section II-C shows that neither GC labeling nor SP labeling completely specifies the worst-case mapping (or the edge profile).

A. Worst-Case Mappings and the Edge Profile

For our analysis, constellations are fully connected, weighted graphs in which the constellation points are the vertices. Fig. 1 shows an example of such a graph for a 4-PAM constellation, with arcs indicating each edge. Note that the self-loop edges are included in the graph. When the constellation is labeled, each of the 2^n vertices has an n -bit label. Then each edge has both a label and a weight. The edge label is the exclusive-or (binary difference) of the labels of two vertices connected by the edge. The edge weight is equal to the Euclidean distance between the two corresponding vertices (or zero for the self-loop edges). For convenience, we assume that normalization forces the smallest Euclidean distance to be one.

A **valid** 2^n -point constellation labeling is simply an n -bit labeling that gives each point a unique label. A valid PAM labeling

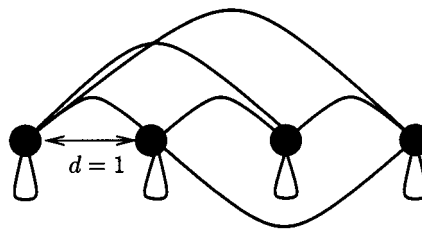


Fig. 1. 4-PAM constellation with arcs indicating all edges.

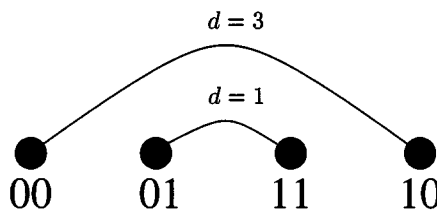


Fig. 2. GC labeled 4-PAM. Arcs indicate edges with edge label 10.

may be described (except for the choice of the zero point) by a **difference list** L . This list includes only the edge labels between neighboring points (which we will call difference labels), starting at the leftmost point and moving to the rightmost point. $L = [01 \ 10 \ 01]$ for the GC-labeled 4-PAM constellation in Fig. 2. By definition, GC labeling implies that the difference list consists of only unit-Hamming-weight difference labels.

The point labels comprise a binary vector space over $GF(2)$. Hence, the difference list must contain a basis for this vector space. The labeling structure may be examined without fixing the basis by using indeterminate basis vectors b_i . $L = [b_1 \ b_2 \ b_1]$ is a basis-independent difference list for Fig. 2.

We similarly define the difference list for a PSK constellation as the list of edge labels between neighboring points starting from any point and moving around the circle until returning to the starting point. When considering PAM and PSK difference lists for the same number of points, the PSK difference list includes one more difference label to complete the circle. If we take $C = [00 \ 01 \ 11 \ 10]$ to be the point-labels of a 4-PSK constellation, the difference list is $L = [01 \ 10 \ 01 \ 10]$ or $L = [b_1 \ b_2 \ b_1 \ b_2]$. Unlike PAM, the choice of starting point for PSK is arbitrary, so any cyclic shift of a PSK difference list is also a valid difference list for that PSK constellation.

Generally, edge labels do not uniquely identify Euclidean distances. For example, the edge label $b_2 = 10$ in Fig. 2 corresponds to edges with Euclidean distances 1 and 3. These are the edges indicated by arcs in Fig. 2. The **worst-case mapping** M gives the minimum distance associated with each edge label. For the example in Fig. 2

$$M = \begin{bmatrix} 00 & 01 & 10 & 11 \\ 0 & 1 & 1 & 2 \end{bmatrix}. \quad (1)$$

Our analysis focuses on the distances in mappings M without listing the corresponding edge labels. This listing, denoted by P , is the **edge profile** of a labeled constellation. For the 4-PAM example in Fig. 2, $P = [0 \ 1 \ 1 \ 2]$.

B. Worst-Case Mappings and Free Distance

Now we investigate the effect of the constellation labeling on the free Euclidean distance of TCM. To begin, consider the ways in which two TCMs might be considered equivalent. Two TCMs are **strictly equivalent** if they implement the same mapping of input information sequences to constellation point sequences. Two TCMs are **range-equivalent** if they have the same set of possible constellation point sequences. Range equivalence is the notion of equivalence used by Forney in [4]. Finally, two TCMs are **distance-equivalent** if they have the same set of worst-case distance sequences, where the **worst-case distance sequences** of a TCM are the distance sequences produced by applying the worst-case mapping M to each binary symbol error sequence produced by an incorrect path through the trellis of the convolutional encoder.

In general, the worst-case distance sequences may be overly pessimistic, i.e., not achievable by an actual trellis error event. However, in the original paper on TCM [3], Ungerboeck showed that the worst-case distance sequences do occur for rate- $k/(k+1)$ TCM. These results can be extended using the equivalence-class encoder analysis introduced in [5] to most rate- $k/(k+2)$ codes, when the constellation has two reflection symmetries and hence can be decomposed into equivalence classes with at least four points each. This condition is satisfied by all the common two-dimensional (2-D) labelings. Whenever all the worst-case distance sequences do occur, those sequences are sufficient to compute the minimum Euclidean distance and the minimum product distance [6], [7] of the trellis code. Thus, in many common situations, distance equivalence alone is enough to establish that two codes have the same values of free Euclidean distance and product distance.

Now we extend the three definitions of equivalence from trellis codes to constellations. Two labeled constellations are strictly, range- or distance-equivalent if any trellis code using one of the constellations with a linear convolutional encoder has a corresponding strictly, range- or distance-equivalent trellis code using the other constellation with a linear convolutional encoder having the same number of memory elements as the encoder of original trellis code.

Considering labels (of points or of edges) as vectors over $GF(2)$, two different labelings of a set of points or a set of edges are **linearly equivalent** if they are related by a linear transformation over the $GF(2)$ vector space of the binary labels. Linearly equivalent point labelings induce strictly equivalent constellations. Linearly equivalent edge labelings induce distance equivalent labeled constellations. Constellations with linearly equivalent edge labelings will have linearly equivalent point labelings if and only if they assign the zero label to the same point.

Worst-case mappings induce a partial ordering on labeled constellations. We say that worst-case mapping M_1 dominates M_2 if the distance mapped by M_1 to each edge label is greater or equal to the distance mapped by M_2 , with at least one strict inequality. One labeled constellation is **distance-superior** to another if it has a worst-case distance mapping that dominates that of the other. A distance-superior constellation leads to strictly better worst-case distance sequences. As discussed earlier, this often implies that one constellation dominates the other in terms

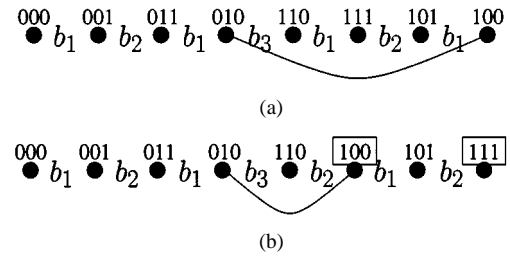


Fig. 3. Two GC 8-PAM constellations with different worst-case distance mappings. Difference labels are indicated by $b_1 = 001$, $b_2 = 010$, and $b_3 = 100$. The arcs identify minimum distance edges with edge label 110. (a) Distance-superior GC 8-PAM. (b) Distance-inferior GC 8-PAM. The two points with labels different from the labeling of (a) are shown in boxes.

of the minimum Euclidean distance and product distance that will result from an exhaustive search of linear convolutional encoders of a fixed complexity.

C. Different Structures Within the Common Paradigms

The following examples demonstrate structurally distinct labelings within both of the standard paradigms (GC and SP) by showing that one labeling is distance-superior to another. Fig. 3 shows two slightly different GC labelings for 8-PAM.

As shown below, the worst-case mappings of Fig. 3(a) and (b) are distinct

$$M(3(a)) = \begin{bmatrix} 000 & 001 & 010 & 100 & 011 & 101 & 111 & 110 \\ 0 & 1 & 1 & 1 & 2 & 2 & 3 & 4 \end{bmatrix}$$

$$M(3(b)) = \begin{bmatrix} 000 & 001 & 010 & 100 & 011 & 101 & 111 & 110 \\ 0 & 1 & 1 & 1 & 2 & 2 & 3 & \mathbf{2} \end{bmatrix}.$$

The different distances associated with $b_2 \oplus b_3 = 110$ cause Fig. 3(a) to be distance-superior to Fig. 3(b). This distance superiority makes constellation in Fig. 3(a) the preferred in exhaustive code searches optimizing Euclidean distance or product distance.

Fig. 4 shows two SP labelings for 16-PAM. The labeling in Fig. 4(a) is the natural labeling, a well-known SP labeling for PAM. The labeling in Fig. 4(b) switches the bit labeling used on the partition of the coset $\{0001, 1001\}$ into two single-point cosets. The worst-case distance mappings are given below for Fig. 4(a) (top) and Fig. 4(b) (bottom) using hexadecimal representation for the binary edge labels

$$\begin{bmatrix} 0 & 1 & 3 & 7 & f & 2 & 6 & e & 5 & d & 4 & c & b & a & 9 & 8 \\ 0 & 1 & 1 & 1 & 1 & 2 & 2 & 2 & 3 & 3 & 4 & 4 & \mathbf{5} & \mathbf{6} & \mathbf{7} & 8 \\ 0 & 1 & 3 & 7 & f & 2 & 6 & e & 5 & d & 4 & c & b & a & 9 & 8 \\ 0 & 1 & 1 & 1 & 1 & 2 & 2 & 2 & 3 & 3 & 4 & 4 & \mathbf{1} & \mathbf{2} & \mathbf{1} & 8 \end{bmatrix}.$$

The 16-PAM SP with point labeling in Fig. 4(a) is distance-superior to the one in Fig. 4(b), providing more distance for the three edge labels $\{b, a, 9\}$. Note that two of these three edge labels are the nonbasis difference labels $e_1 = 9$ and $e_2 = b$ that appear in Fig. 4(b) but not in Fig. 4(a). With a standard additive white Gaussian noise (AWGN) trellis code, the distance-superior labeling provides a bit error rate advantage at low signal-to-noise ratio (SNR). Similar examples are given in [8] for GC 8-PSK and SP 16-QAM.

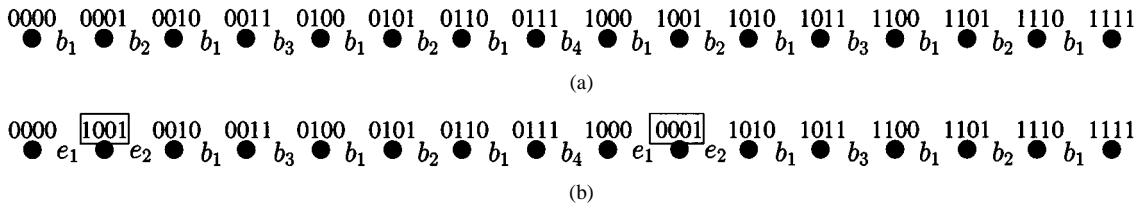


Fig. 4. Two set-partition-labeled 16-PAM constellations with different worst-case distance mappings. Difference label basis vectors are indicated by $b_1 = 0001$, $b_2 = 0011$, $b_3 = 0111$, and $b_4 = 1111$. (a) Distance-superior SP-labeled 16-PAM. (b) Distance-inferior SP-labeled 16-PAM. The two points with labels different from (a) are shown in boxes. The non-basis difference labels are $e_1 = b_1 \oplus b_3 \oplus b_4$ and $e_2 = b_2 \oplus b_3 \oplus b_4$

III. LABELINGS WITH UNDOMINATED EDGE PROFILES

When comparing one edge profile to another, it is helpful to sort the elements in each profile. Let angle brackets indicate that the elements of an edge profile are sorted to increase monotonically. Thus, while the elements of P may be in any order, the elements of $\langle P \rangle$ must increase monotonically.

Edge profile P_1 **dominates** P_2 if the value in every position of $\langle P_1 \rangle$ is greater or equal to the value in the corresponding position of $\langle P_2 \rangle$, with at least one strict inequality. An edge profile is **undominated** if no valid constellation labeling produces an edge profile that dominates it. This section presents the SU labeling structure and proves that its edge profile is undominated.

Section III-A introduces the SU labeling structure for PAM constellations. Section III-B shows that SU PAM has an undominated edge profile. Section III-C extends the SU structure to PSK and square QAM, again showing that SU labeling results in an edge profile that is undominated. Section III-D demonstrates how to select the difference label basis so that SU labeling can meet either the GC or the SP paradigm.

An edge profile may be undominated but still not dominate all other edge profiles; there is still the possibility that another labeling has a sorted profile that is better in some places and worse in others, such that neither edge profile dominates the other. Section III-E explores when the SU edge profile dominates all others.

A. SU Labeling

Gilbert's taxonomy of Gray codes [9] enumerates a number of different labeling structures that meet the GC condition and classifies them according to structure. In particular, Gilbert identifies composite and ultracomposite Gray codes. Below, we extend Gilbert's definitions of composite and ultracomposite GC difference lists to permit basis vectors with Hamming weight larger than 1. We also consider the special case (defined below) of SU difference lists. Later, we show that SU difference lists provide undominated edge profiles.

Let A and B be two valid difference lists for 2^{n-1} -PAM, as L in Section II-A, each containing $(2^{n-1} - 1)$ difference labels drawn from a set of indeterminate basis vectors $\{b_1, \dots, b_{n-1}\}$. The basis vectors of A and B both must span the $n - 1$ dimensional binary space, but they need not be identical. As valid difference lists, A and B must provide valid labelings of 2^{n-1} -PAM when the indeterminate basis vectors are set to $(n - 1)$ -bit basis vectors. Let b_n be an indeterminate basis vector that extends the range of the bases in A and B to the full n -dimensional binary space. For a 2^n -PAM constellation,

$\{A, b_n, B\}$ is called a **composite** difference list. Let C_n be the set of all composite difference lists for 2^n -PAM constellations.

Such composite difference lists always provide valid 2^n -PAM constellation labelings when the indeterminate basis vectors are set to n -bit basis vectors. This general truth may be readily understood by considering a special case. Let the leftmost point be labeled with all zeros. Let $\{b_1, \dots, b_{n-1}\}$ have a zero in the most significant bit (MSB), and let b_n be all zeros except the MSB. Ignoring the MSB, the resulting constellation labeling is a concatenation of two valid labeled 2^{n-1} -PAM constellations, one according to A , and the other according to B . Considering the MSB, the left 2^{n-1} -PAM constellation has the MSB = 0, and the right 2^{n-1} -PAM constellation has the MSB = 1.

The set U_n of **ultracomposite** difference lists for 2^n -PAM is constructed by induction. The base case U_1 is simply $\{[b_1]\}$. Given U_{n-1} , U_n contains the composite difference lists constructed by connecting two (possibly identical) difference lists from U_{n-1} . Thus, U_2 contains $[b_1 \ b_2 \ b_1]$. U_n is completed by adding any difference list obtained by permuting the indexes of the indeterminate basis vectors in any difference list already in U_n . Thus,

$$U_2 = \{[b_1 \ b_2 \ b_1], [b_2 \ b_1 \ b_2]\}.$$

In general, $U_n \subseteq C_n$. For 2- and 4-PAM all valid difference labels are ultracomposite and $U_n = C_n$. For 8-PAM, noncomposite difference labels exist, but because all 4-PAM difference labels are ultracomposite we still have $U_8 = C_8$. For 16-PAM and larger, $U_n \subset C_n$.

Symmetric Ultracomposite (SU) difference lists are ultracomposite difference lists where every composite difference list in the construction combines two identical difference lists. The difference lists for SU 2-, 4-, and 8-PAM below illustrate the recursive structure of SU difference lists.

$$b_1 \tag{2}$$

$$b_1 \ b_2 \ b_1 \tag{3}$$

$$b_1 \ b_2 \ b_1 \ b_3 \ b_1 \ b_2 \ b_1 \tag{4}$$

$$\vdots \tag{5}$$

The commonly used reflected binary labeling structure in Gray's 1953 patent [1] is SU with unit-Hamming-weight difference labels b_i . However, for the general SU structure, b_1, \dots, b_n can be any basis of n linearly independent n -bit difference labels. Looking back at Fig. 3(a) and (b), both are ultracomposite, but only Fig. 3(a) is SU. Furthermore, Fig. 4(a) is SU, but Fig. 4(b) is not even composite.

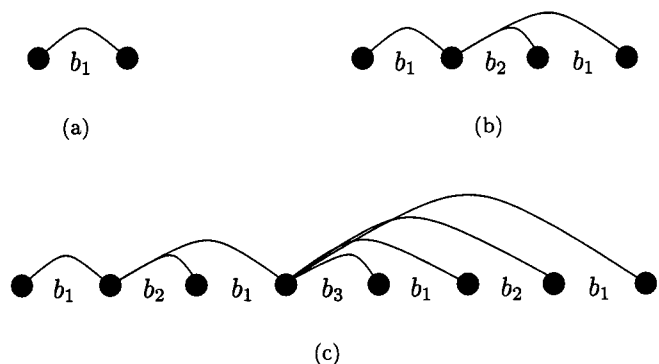


Fig. 5. For each SU labeled constellation above, arcs indicate minimum distance edges for each edge label. These arcs illustrate how the edge profile of 2^n -PAM inherits the edge profile of 2^{n-1} -PAM.

The difference list for SU 2^n -PAM is simply two SU 2^{n-1} -PAM difference lists connected by a central b_n . As a result, the worst-case mapping and edge profile for SU 2^n -PAM includes that of SU 2^{n-1} -PAM. Fig. 5 illustrates how the minimum-distance edges are inherited by the next larger PAM constellation. This figure also shows how central location of the new difference label b_n causes the integers $1, \dots, 2^{n-1}$ to comprise the new elements in the edge profile of SU 2^n -PAM as compared to SU 2^{n-1} -PAM. Equation (6) shows the general form of $P(\text{SU } 2^n\text{-PAM})$. The values to the left of the last comma are the edge profile of 2^{n-1} -PAM.

$$P(\text{SU}) = [0, 1, 12, \dots, 12 \dots 2^{n-2}, 12 \dots 2^{n-1}]. \quad (6)$$

B. SU Edge Profiles Are Undominated

We show that SU difference lists have undominated edge profiles through the recursive application of four lemmas that explore the structural requirements necessary to at least achieve $\langle P(\text{SU } 2^n\text{-PAM}) \rangle$, the sorted version of (6). We will use a running example of 8-PAM. Note that

$$\langle P(\text{SU } 8\text{-PAM}) \rangle = [1 \ 1 \ 1 \ 2 \ 2 \ 3 \ 4].$$

The proof technique works from the ends of $\langle P(\text{SU}) \rangle$ toward the middle. When working on the left end with profile entries of 1 or 2, the goal is to ensure that no more than the number of 1's or 2's in $\langle P(\text{SU}) \rangle$ appear in the edge profile. The fewer small values in the edge profile the better. When working on the right end with profile entries of 2^{n-1} or $2^{n-1} - 1$, the goal is to ensure that at least the number of 2^{n-1} 's or $2^{n-1} - 1$'s in $\langle P(\text{SU}) \rangle$ appear in the edge profile. The more occurrences of large values in the edge profile the better. At each step, we show that it is not possible to do better than $\langle P(\text{SU}) \rangle$, given that up to that point $\langle P(\text{SU}) \rangle$ has been achieved.

Lemma 1: The least number of 1's in an edge profile for 2^n -PAM is n . To have exactly n 1's in the edge profile, the $2^n - 1$ element difference list L must consist of exactly n linearly independent labels $\{b_1, b_2, \dots, b_n\}$.

Proof: L must contain a basis of size n for the point labels. Hence the difference list must contain n linearly independent labels. Since each distinct edge label in the difference list corresponds to a 1 in the edge profile, the lemma is proved. \square

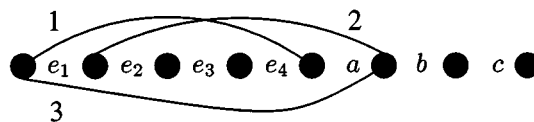


Fig. 6. Illustration for proof of Lemma 2.

We will use b_i to refer to the difference list elements that are also designated as basis vectors in our line of argument. For 8-PAM, call these basis-vector difference labels b_1, b_2 , and b_3 . Note that according to Lemma 1, all difference labels must be basis vectors to achieve the minimum number of 1's in the edge profile. However, there remains considerable freedom as to how these basis-vector difference labels are to be arranged. In the rest of the argument, we use e_i to denote indeterminate difference labels for which we have not yet specified the particular basis vector.

Lemma 2: 2^n -PAM has at most one edge profile entry of 2^{n-1} . To achieve this entry the difference list must have the following repeating structure:

$$L = [e_1 \ e_2 \ \dots \ e_{2^{n-1}} \ e_1 \ e_2 \ \dots \ e_{2^{n-1}-1}]. \quad (7)$$

Proof: The sorted Euclidean distances of the edges emanating from any single point form an upper bound on each element of the sorted edge profile. This is because each of these edges has a distinct edge label.

There is only one edge emanating from the right central point (RCP) with length 2^{n-1} , and no larger edges. This proves that there can be at most one entry in the edge profile with length 2^{n-1} .

The rest of the proof hinges on the length- 2^{n-1} edge from the RCP to the left endpoint. For 8-PAM this edge is indicated by arc 1 in Fig. 6, with length $2^{n-1} = 4$.

Label the first 2^{n-1} difference labels with the indeterminate labels $e_1 \dots e_{2^{n-1}}$, as in Fig. 6 for 8-PAM. By construction, the edge label for the edge from the RCP to the left endpoint is $e_1 \oplus e_2 \oplus \dots \oplus e_{2^{n-1}}$. For 8-PAM this is $e_1 \oplus e_2 \oplus e_3 \oplus e_4$. To have an entry of 2^{n-1} in the edge profile, every point must have an edge labeled $e_1 \oplus e_2 \oplus \dots \oplus e_{2^{n-1}}$ with distance 2^{n-1} or more.

Consider the point just to the right of the RCP. The only edge of length 2^{n-1} or larger that can be labeled $e_1 \oplus e_2 \oplus \dots \oplus e_{2^{n-1}}$ is the length 2^{n-1} edge emanating to the left, arc 2 in Fig. 6. (Arc 3 has sufficient length, but its edge label cannot be $e_1 \oplus e_2 \oplus e_3 \oplus e_4$.) This forces $a = e_1$. Working to the right in the same way, the rest of the difference labels are forced to follow the lemma, $b = e_2$ and $c = e_3$ in the example of Fig. 6. \square

Note that Lemma 2 does not preclude $e_i = e_j$ when $i \neq j$. Lemma 3 places some restrictions on when $e_i = e_j$ can hold.

Lemma 3: Assuming the structure of Lemmas 1 and 2, 2^n -PAM must have at least $n - 1$ entries of 2 in its edge profile. To have only $n - 1$ such entries, $e_i = e_j$ is only possible when i and j are either both even or both odd.

Proof: Fig. 7 shows the difference labeling structure resulting from Lemma 2 for 8-PAM with arcs added to identify all the length-2 edges. The points connected by the top arcs produce a constellation of half the original size. As in the proof of

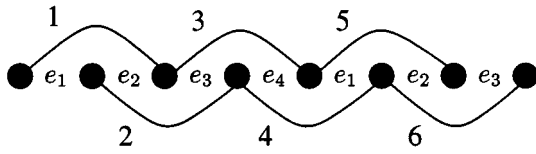


Fig. 7. Illustration for proof of Lemma 3.

Lemma 1, for these 2^{n-1} points to have distinct labels, there must be at least $n - 1$ distinct, linearly independent edge labels for the top arcs. This proves that $n - 1$ is a lower bound on the number of length-2 edge labels, except if one of the length-2 edge labels were also a length-1 edge label.

If the same label were to appear on both length-1 and length-2 edges, this edge label would be both a length-1 edge label and the binary addition of two length-1 edge labels. This would violate the requirement of Lemma 1 that distinct length-1 edge labels (difference labels) be linearly independent. Thus, if the labeling obeys the structure of Lemmas 1 and 2, $n - 1$ is a lower bound on the number of length-2 edge labels. (SU labeling achieves this lower bound).

Now we work from the left setting $e_i = e_j$ whenever possible while labeling the arcs in Fig. 7 to have exactly $n - 1$ distinct labels. The leftmost arc is arc 1, which has label $e_1 \oplus e_2$. The first and third points must have distinct labels. Thus, $e_1 \neq e_2$.

We wish to have exactly $n - 1$ distinct labels for length-2 edges. One such label is $e_1 \oplus e_2$. We now have $n - 2$ unspecified length-2 labels and $n - 2$ unused distinct difference labels (assuming from Lemma 1 that there are only n distinct difference labels). Thus, we may introduce a new length-2 edge label only when a previously unused difference label appears.

The arc 2 label of $e_2 \oplus e_3$ is either an already used length-2 label (forcing $e_3 = e_1$) or e_3 must be distinct from e_1 and e_2 . Similarly, the arc 3 label of $e_3 \oplus e_4$ is either an already used label forcing $e_4 = e_2$ or a new length-2 label forcing e_4 to be a new edge label. While the example shows only 8-PAM, this pattern continues for any 2^n -PAM constellation, enforcing the lemma. \square

Lemma 4: Assuming the structure of Lemmas 1–3, 2^n -PAM has at most one entry of $(2^{n-1} - 1)$ in its edge profile. To achieve this entry, $e_i = e_j$ must hold either for all even i and j or all odd i and j .

Proof: Given the structure of Lemmas 1–3, there are only two possibilities for an edge profile entry of $(2^{n-1} - 1)$. Arcs 1 and 2 in Fig. 8 illustrate these two possibilities for 8-PAM. Note from Lemma 2 that arc 3 in Fig. 8 is unavailable; it already provides an edge profile entry of (2^{n-1}) . As we see below, arc 1 and arc 2 cannot simultaneously provide edge profile entries of $(2^{n-1} - 1)$, hence only one such entry is possible.

The rest of the argument is analogous to that of Lemma 2 but considers how to have an edge label with minimum distance $2^{n-1} - 1$ rather than 2^{n-1} . We describe the conclusions without repeating the argument details.

There are two cases to consider. For the first case, assume that arc 1 of Fig. 8 provides the edge profile entry of $(2^{n-1} - 1)$, i.e., the label $e_1 \oplus e_2 \oplus \dots \oplus e_{2^{n-1}-1}$ has minimum distance $2^{n-1} - 1$. With arguments similar to the proof of Lemma 2, this forces $e_i = e_j$ for all even i and j . Note that with this condition, the

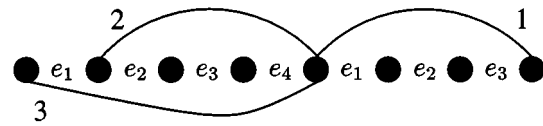


Fig. 8. Illustration for proof of Lemma 4.

label of arc 2 simplifies to e_3 in Fig. 8. The minimum distance mapped to e_3 is 1. More generally, the label $e_2 \oplus e_3 \oplus \dots \oplus e_{2^{n-1}}$ must have minimum distance $(2^{n-1} - 3)$ or less.

For the second case assume that arc 2 provides the edge profile entry of $(2^{n-1} - 1)$, i.e., the label $e_2 \oplus e_3 \oplus \dots \oplus e_{2^{n-1}}$ has minimum distance $2^{n-1} - 1$. Again, with arguments similar to the proof of Lemma 2, this forces $e_i = e_j$ for all odd i and j . As in the first case, the label of the other distance- $(2^{n-1} - 1)$ edge (arc 1 in this case) simplifies to an edge label (e_2 in Fig. 8) with minimum distance $(2^{n-1} - 3)$ or less. These two cases are the only two ways to have an edge label with minimum distance $2^{n-1} - 1$, and they are mutually exclusive. \square

Lemma 4 instructs us to replace with b_1 either all e_i with i even or all e_i with i odd. Essentially, we place b_1 in every other position of the difference list. We are now ready to show that SU-PAM is undominated.

Theorem 1: For 2^n -PAM, $P(\text{SU})$ is undominated.

Proof: For our 8-PAM example, the structure of Lemmas 1–4 completely determines the edge profile to be the SU edge profile

$$\langle P \rangle = [0 \ 1 \ 1 \ 1 \ 2 \ 2 \ 3 \ 4].$$

Also, because there must be exactly three linearly independent difference labels, Lemmas 1–4 fully describe the difference list structure to be either

$$[b_1 \ b_2 \ b_1 \ b_3 \ b_1 \ b_2 \ b_1] \quad (8)$$

or

$$[b_2 \ b_1 \ b_3 \ b_1 \ b_2 \ b_1 \ b_3]. \quad (9)$$

For larger PAM constellations, the labeling freedom remaining after the placement of the b_1 's may be considered in terms of labeling the difference labels of the 2^{n-1} -PAM subconstellation produced by ignoring every other point of the original 2^n -PAM constellation.

Appendix A examines the relationship between the edge profile of the subconstellation and that of the original constellation. This relationship indicates that for the original constellation to at least achieve the SU edge profile, Lemmas 1–4 must apply to the subconstellation.

Thus, we force every other position of the subconstellation difference list to be equal by placing b_2 in every other open (non- b_1) position of the original difference list. Continuing in this manner, after placing b_1, \dots, b_i we place b_{i+1} in every other open position in the difference list.

As in the 8-PAM example above, the resulting labeling always has exactly the SU edge profile. Since improvement over the SU edge profile was impossible with each application of a lemma, the theorem is proved. \square

The recursive procedure in the proof of Theorem 1 produces exactly the SU edge profile. Depending on the placement of

the first b_1 difference label, the procedure yields either the SU labeling or a shifted version of the SU labeling, which is not SU. Appendix A provides a more detailed examination of the recursive application of Lemmas 1–4 and provides an example for 32-PAM.

C. PSK and Square QAM

Theorem 1 easily extends to demonstrate the optimality of SU labelings for 2^n -PSK constellations. For PSK, cyclically shifting the difference list is not structurally significant and the procedure always produces an SU labeling.

Now consider 2^{2n} -QAM constellations. For 2^{2n} -QAM, we seek an undominated edge profile that has $2n$ entries of 1. (An extension of Lemma 1 shows that this is the smallest number possible.) Through a change of basis, any such labeling has edge labels linearly equivalent to those of a GC labeling. Thus, we begin with a lemma about the structure of GCs for rectangular constellations. Our immediate concern is squares, but Section IV will use the more general result.

Lemma 5: The only ways to GC label a $(2^n \times 2^m)$ -point rectangular constellation are direct products of a GC- 2^n -PAM and a GC- 2^m -PAM.

Proof: First we define the direct product labeling structure. To construct a direct product of two PAM constellations, first augment the 2^m -point horizontal PAM and the 2^n -point vertical PAM point labels (or difference labels) to have $m + n$ bits. The direct product is then produced by labeling each point in the QAM constellation with the binary addition of the corresponding horizontal and vertical point labels.

A simple example of this procedure is to augment a vertical GC-PAM by adding zeros to the left and a horizontal GC-PAM by adding zeros to the right. Then the final QAM labeling will also be GC. Section III-D gives an example of a direct product construction of SP labeling.

The augmentation of the point labels (or difference labels) may be accomplished in any way that satisfies two conditions. It must preserve the basis-independent difference list of each PAM (hence preserving the PAM edge profile), and it must produce $m + n$ linearly independent difference labels: m from the horizontal PAM and n from the vertical PAM. This second condition ensures that each constellation point has a distinct label. A rectangular constellation is labeled with such a direct product structure if and only if each horizontal 2^m -PAM subconstellation has the same difference list and each vertical 2^n -PAM subconstellation has the same difference list.

Of course, to construct a GC rectangular constellation as the direct product of two GC-PAM constellations the augmentation must satisfy a third condition. The augmented difference lists must contain only unit Hamming-weight difference labels. The direct product structure implies linear equivalence to a GC labeling since we can obtain a GC labeling from any direct-product labeling through a change of basis.

Now we show that GC labeling requires the direct product structure. First note that to GC-label any rectangle, each vertical PAM and each horizontal PAM subconstellation in the rectangle must be GC-labeled. Consider any four neighboring points as illustrated in Fig. 9. The four edges connecting these points form a

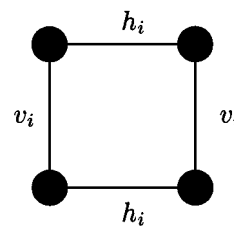


Fig. 9. Four neighboring points within a larger GC-labeled rectangle of points.

cycle, hence the binary sum of the four corresponding difference labels must be zero. If each of these difference labels must also have unit Hamming weight, the only possible labeling structure is that of Fig. 9 where the horizontal difference labels are identical and the vertical difference labels are identical.

Considering an entire row of such four-point cycles, all the vertical difference labels in a row must be identical in any GC-labeled rectangle. Similarly, all the horizontal difference labels in a column must be identical. As a result, every horizontal 2^m -PAM has the same difference list and every vertical 2^n -PAM has the same difference list. Hence the labeling has the direct product structure. \square

We have just shown that all the direct products of GC-PAMs have the minimum number of 1's in the edge profile, but they do not all have undominated edge profiles. To see how to ensure an undominated QAM edge profile, we first discuss how the edge profile of a direct-product QAM constellation is related to its parent PAM constellations. To maintain integer values, it is convenient here to refer to the squared edge profile as P^2 , so that for our 4-PAM example with $\langle P \rangle = [0 \ 1 \ 1 \ 2]$ we have

$$\langle P^2(\text{SU 4-PAM}) \rangle = [0 \ 1 \ 1 \ 4]. \quad (10)$$

Using the Pythagorean theorem, the squared edge profiles for 2^{2n} -point QAM labelings resulting from the direct product of two 2^n -PAM labelings consists of all the pairwise sums of elements, one from each edge profile. For example, suppose we construct a 16-QAM labeling as the direct product of two SU 4-PAM labelings. The resulting squared edge profile can be computed from the following matrix of pairwise sums:

	0	1	1	4
0	0	1	1	4
1	1	2	2	5
1	1	2	2	5
4	4	5	5	8

The edge profile $\langle P^2(\text{SU 16-QAM}) \rangle$ is

$$\langle P^2 \rangle = [0 \ 1 \ 1 \ 1 \ 1 \ 1 \ 2 \ 2 \ 2 \ 2 \ 4 \ 4 \ 5 \ 5 \ 5 \ 5 \ 8]. \quad (11)$$

Theorem 2: The direct product of two SU PAM constellations produces a QAM constellation with an undominated edge profile.

Proof: Every constellation that has the minimum number of 1's in the edge profile is linearly equivalent to a GC labeling. Lemma 5 shows that such GC-labeled constellations have the direct product structure. Hence, non-direct-product QAMs cannot dominate direct-product QAMs; they have two many 1's in the edge profile.

Within the direct-product structure, the relationship of the QAM edge profile to the parent PAM edge profiles guarantees that the QAM edge profile will be undominated if and only if the parent PAM edge profiles are undominated. Hence, one class of QAM labelings with undominated edge profiles are those labelings produced by taking the direct product of two SU-PAM labelings. We call such labeling an SU-QAM labeling. \square

D. SU-GC and SU-SP Labeling

For PAM, PSK, and square QAM, choosing any basis of unit Hamming-weight difference labels produces SU labelings that are also GC labelings. With the proper choice of basis, an SU labeling can also produce an SP labeling. For PAM and PSK constellations using the SU construction in (2)–(5), setting b_i to be the basis vector with ones in the i least significant positions and zeros elsewhere produces an SU labeling that is also SP. For example, an SU-SP labeling for 4-PAM has $L = [01 \ 11 \ 01]$. Fig. 4(a) gives such an SU-SP labeling for 16-PAM.

For 2^{2n} -point square QAM constellations, an SU-SP labeling can be constructed by simple augmentations to $2n$ bits of the n -bit basis vectors for SU-SP 2^n -PAM discussed above. One of the constituent PAM bases expands each basis vector by inserting n zeros, one to the left of each of the n original bits. The other constituent PAM basis replaces each of the n original bits with that bit value repeated twice. As an example, an SU-SP labeling of 16-QAM may be constructed from the 4-PAM difference list above as the direct product of two 4-PAM labelings, one with $L = [0001 \ 0101 \ 0001]$ and the other with $L = [0011 \ 1111 \ 0011]$. For a proof of how this direct product structure always produces SP labeling, see [8, Theorem 9].

The SU labelings for GC and SP differ only in the choice of bases. This demonstrates that for all 2^{2n} -point square-QAM and all 2^n -point PAM and PSK constellations there exist linearly equivalent SP and GC labelings. This fact was also established in [8, Theorem 9]. When such SU labelings are employed (and they are the commonly used SP and GC labelings), there is no difference between the trellis codes possible using linear convolutional codes with the GC labeling and those possible using linear convolutional codes with the SP labeling. In contrast, our results in Section II demonstrated examples where two constellations, both GC-labeled or both SP-labeled, could produce distinct sets of trellis codes (having distinct worst-case distance sequences). Neither the GC nor the SP paradigm specifies the underlying structure as precisely as the SU paradigm.

E. When Do SU Profiles Dominate All Others?

Theorems 1 and 2 prove only that SU labelings are undominated. There remains the possibility that another labeling has a sorted profile that is better in some places and worse in others. The next theorem shows that if such an occurrence is possible at all for PAM, the labeling that achieves it is not ultracomposite.

Theorem 3: The SU labeling for 2^n -PAM has an edge profile that equals or dominates the edge profiles of all other ultracomposite labelings.

Proof: For a two-point constellation, the theorem clearly holds. Now suppose that it holds for 2^{n-1} -PAM. Recall that the sorted Euclidean distances of the edges emanating from any

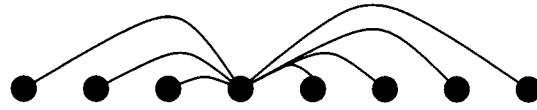


Fig. 10. Arcs in an edge profile bound for 8-PAM.

single point form an upper bound on each element of the sorted edge profile. Construct such a bound using the left of the two central points in a 2^n -PAM constellation. The arcs in Fig. 10 indicate the edges in such a bound for 8-PAM. The bound is

$$\langle P \rangle < [0 \ 1 \ 1 \ 2 \ 2 \ 3 \ 3 \ 4]. \quad (12)$$

Now note that if we assume that our 2^n -point constellation has an ultracomposite labeling, the 2^{n-1} points on the left have a basis-independent difference list that would provide a valid ultracomposite labeling of that 2^{n-1} -PAM constellation. Hence, the edge profile for ultracomposite 2^{n-1} -PAM is upper-bounded by the edge profile of SU 2^{n-1} -PAM. Now we can tighten the upper bound of (12) by replacing values associated with the arcs between points in the left 2^{n-1} -PAM constellation with the values of the SU 2^{n-1} -PAM edge profile, which were shown in Fig. 5. Thus, we can replace entries $\{0, 1, 2, 3\}$ in (12) with $\{0, 1, 2, 2\}$. This yields the tighter bound

$$\langle P \rangle < [0 \ 1 \ 1 \ 1 \ 2 \ 2 \ 3 \ 4]. \quad (13)$$

Notice that (13) is exactly the edge profile of SU 8-PAM illustrated in Fig. 5(c). In general, this tighter bound is exactly the edge profile of SU 2^n -PAM. The SU-labeling structure has an edge profile that equals or dominates every ultracomposite labeling because it achieves this tighter upper bound. \square

Still, Theorem 3 leaves open the possibility of non-ultracomposite labelings with edge profiles that are better in some positions than the SU labeling. Note that all 2-, 4-, and 8-PAM constellations are ultracomposite. In [8] we showed that such an occurrence is impossible for the smallest 2-D constellations, 4-PSK, 8-PSK, and 16-QAM. However, whether or not SU labelings have edge profiles that dominate all others in general remains an open question.

IV. CROSS CONSTELLATIONS

We now turn our attention to cross constellations. This section focuses attention on the standard cross constellations with 32 or more points, i.e., 2^{2n+1} -QAM constellations with $n > 1$. Fig. 11 shows how such cross constellations have a central $2^n \times 2^n$ square with four wings, each a $2^n \times 2^{n-2}$ rectangle. The central square and right and left wings comprise a $2^n \times 3 \cdot 2^{n-1}$ central rectangle.

The standard 8-QAM constellation is also considered a cross constellation, but it lacks the central-square-with-four-wings structure. This structural difference leads to different labeling properties. Appendix B shows that all SP labelings of 8-QAM have the best possible edge profile for 8-QAM. In the rest of this section, we use the phrase “cross constellation” to denote constellations that have the structure of Fig. 11, i.e., 32-cross and larger.

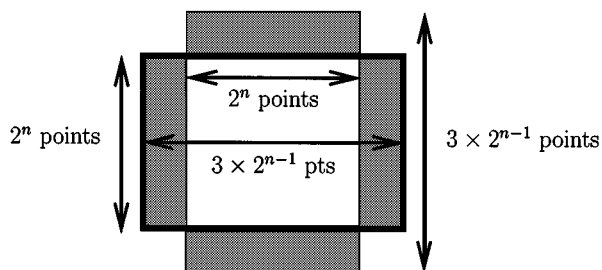


Fig. 11. A 2^{2n+1} cross constellation. The unshaded region is the central square. The wings are shown as shaded rectangles. The central rectangle is outlined in bold.

Section IV-A shows that cross constellations cannot be Gray labeled. Section IV-B presents a procedure that produces quasi-Gray-labeled cross constellations by approximating the SU structure. We call this labeling structure quasi-SU. Section IV-C shows that these quasi-SU cross constellations have fewer 1's in the edge profile than standard SP-labeled cross constellations. However, the SP cross constellations are still the best choice for trellises with parallel branches. Some example code searches demonstrate how the choice between SP and quasi-SU hinges on the presence of parallel branches in the trellis.

A. Cross Constellations Cannot Be GC-Labeled

In this subsection, we establish that cross constellations require $2n + 2$ minimum-distance edge labels (difference labels) rather than the $2n + 1$ difference labels characteristic of a GC labeling.

Theorem 4: All 2^{2n+1} cross constellations must have at least $2n + 2$ difference labels.

Proof: It is sufficient to show that the constellation cannot be GC-labeled. The arguments of Lemma 5 show that to GC-label the central rectangle alone, all the horizontal $3 \cdot 2^{n-1}$ -PAM difference lists must be identical and all the vertical 2^n -PAM difference lists must be identical. Furthermore, the horizontal difference labels must be distinct from the vertical difference labels.

The horizontal $3 \cdot 2^{n-1}$ -PAM difference list requires $n+1$ distinct Hamming-weight-one labels, and the vertical 2^n -PAM difference list requires an additional n such labels. Thus, all $2n+1$ unit-Hamming-weight labels have been used. Now consider labeling the first row of points in either the top or bottom wing. The structure of the GC-labeled central rectangle makes it impossible to label even these 2^n points distinctly while using only Hamming-weight-one edges between neighboring points.

Fig. 12 illustrates this situation for 32-QAM. The difference labels $v_1, v_2, h_1, h_2,$ and h_3 are the five distinct unit-Hamming-weight difference labels. These difference labels are used to label the 4×6 central rectangle. Difference label e_1 cannot be v_1 or v_2 without forcing two points, (a, b) and (a, c) , respectively, to have the same label. Similarly, e_1 cannot be equal to h_1 or h_2 , and e_2 cannot be equal to h_1 or h_3 .

For a GC-labeling, e_1 and e_2 need to have the same label in order to allow e_3 to have unit Hamming weight (by being h_1). At this point, we see that there are no options for e_1

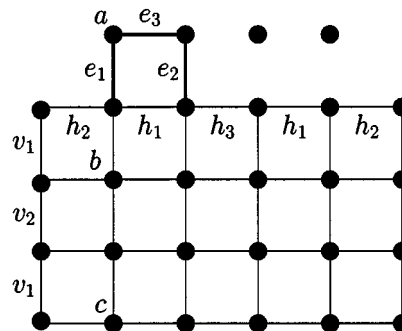


Fig. 12. Illustration of why 32-QAM cannot be GC-labeled.

that support GC-labeling since it cannot take on any of the unit-Hamming-weight labels. Similar arguments apply to any 2^{2n+1} -QAM cross constellation with $n > 1$. \square

B. Quasi-SU Cross Constellations

Motivated by the undominated edge profile provided by SU-labeled 2^{2n} -QAM, we label cross constellations by manipulating SU-labeled rectangular constellations. The next theorem provides a construction that requires exactly one extra minimum-distance edge, which is the best that can be expected given Theorem 4. Such a labeling is commonly called a quasi-Gray labeling when $2n + 1$ of the $2n + 2$ difference labels have unit Hamming weight.

Theorem 5: All 2^{2n+1} cross constellations may be labeled to have $2n + 2$ difference labels.

Proof: The $n=1$ case is demonstrated in Appendix B. For $n > 1$ this proof provides a constructive procedure that proves the theorem. First, construct an SU labeled $2^n \times 2^{n+1}$ -point “wide” rectangle as a direct product of two SU-labeled PAM constellations. Fig. 13(a) shows the SU labeled rectangle with vertical difference labels $SU(v_1, v_2, \dots, v_n)$ and the horizontal difference labels $SU(h_1, h_2, \dots, h_{n+1})$. The unshaded $2^n \times 3 \cdot 2^{n-1}$ central rectangle of Fig. 13(a) is exactly the labeled central rectangle of our final cross constellation.

Now we construct the $2^{n-2} \times 2^{n-1}$ “wide” rectangle comprising the right half of the top wing as an SU-labeled rectangle. Considering this rectangle as a separate SU-labeled constellation, the vertical difference labels are $SU(v_2, v_3, \dots, v_{n-1})$. The horizontal difference labels are $SU(h_1, h_2, \dots, h_{n-2}, v_1)$. Note that v_1 appears here as a horizontal edge label. Fig. 14 illustrates for 512-cross how this portion of the top wing consists exactly of those points in the top half of the right shaded rectangle in Fig. 13(a) and (b). The directional arrows in Fig. 14 indicate the order in which points are moved from the shaded rectangle to the top wing.

Now consider how this rectangle (the right half of the top wing) connects to the central rectangle. The left half of this rectangle connects to the central rectangle with vertical edges labeled h_n . The right half of this rectangle connects to the central rectangle with vertical edges labeled $h_n \oplus h_{n-1} \oplus v_1$.

Actually, the entire top wing is an SU-labeled rectangle. The edge labeling of the right half of the wing is reflected to produce that of the left half. The two halves are connected with the difference label h_{n+1} .

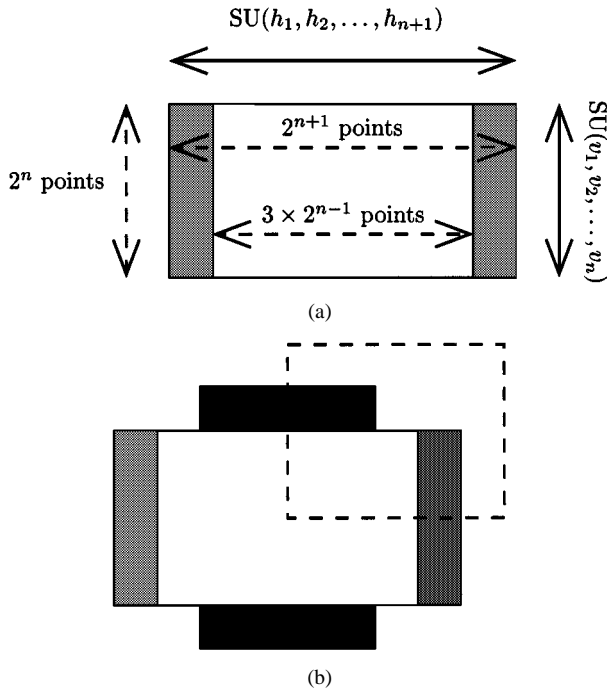


Fig. 13. To construct a quasi-SU cross labeling, points in the right and left shaded regions of the SU labeled rectangle are used to construct the top and bottom wings (shown in black) of the cross constellation. (a) An SU labeled $2^n \times 2^{n+1}$ -point rectangle. (b) Converting an SU rectangle to a quasi-SU cross. The region in the dashed rectangle is shown in detail for quasi-SU 512-cross in Fig. 14.

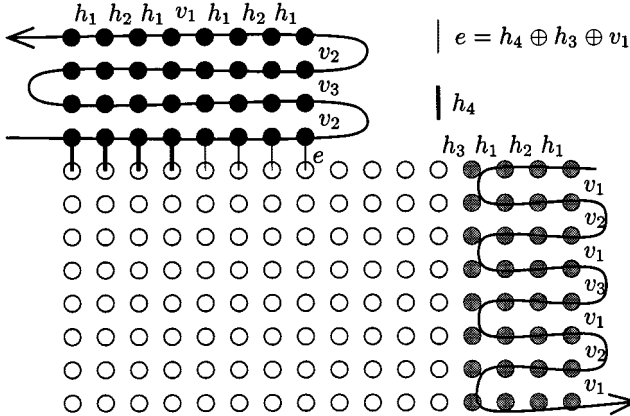


Fig. 14. Detail for quasi-SU 512-cross showing how 32 points are moved from the top right edge of the SU labeled 16×32 -point rectangle to form the right half of the top wing of the cross constellation.

The point labels from the $2^{n-1} \times 2^{n-2}$ rectangle in the top half of the left shaded region of Fig. 13(a) comprise the left half of the top wing. Similarly, the bottom halves of the left and right shaded regions of Fig. 13(a) comprise the left and right halves of the bottom wing, which has an edge labeling that is simply a reflection of the top wing's edge labeling.

This constructive procedure proves the theorem for $n > 1$. The $2n + 2$ difference labels are v_i with $1 \leq i \leq n$, h_i with $1 \leq i \leq n + 1$, and $h_n \oplus h_{n-1} \oplus v_1$. \square

There are other ways to quasi-Gray-label a cross constellation. We distinguish the labeled cross constellations produced by the procedure in the proof of Theorem 5 by calling them

quasi-SU. The quasi-SU construction appears generally to produce a good quasi-Gray labeling since it retains the SU structure except along the interfaces between the central rectangle and the top and bottom wings.

We have performed a complete combinatorial analysis of the 32-cross case and found that quasi-SU 32-cross has an undominated edge profile. This combinatorial analysis considered all possible quasi-Gray labelings of 32-cross. These labelings may be classified into six sets, according to structure. Each of these sets imposes a structure-based upper bound on each position of the sorted edge profile. Quasi-SU 32-cross achieves the upper bound of its structural set, and this upper bound dominates the upper bounds of the other five structural sets. Thus, quasi-SU 32-cross has an edge profile that either equals or dominates the edge profiles of all quasi-Gray labelings. Hence it has an undominated edge profile.

Table I lists the six edge-profile bounds for the six structural sets. Fig. 15 shows, for each of the six structural classes, a labeled 32-QAM constellation that achieves the edge-profile bound for its structural class.

Note that our combinatorial analysis does not rule out the existence of other, structurally distinct, quasi-Gray-labeled 32-QAM constellations beyond these six. Our analysis does ensure that any such constellations will not have better edge profiles. For the details of the combinatorial analysis, we refer the reader to [10], [11].

C. Quasi-SU Versus SP for Cross Constellations

In contrast to the 2^{2n} -QAM case where SU labeling supports SP labeling, no 2^{2n+1} -QAM constellations with $n > 1$ can be both quasi-SU and SP. There is a structural difference between SP labeling and quasi-SU labeling.

As a specific example of this fact, consider 32-cross. The top row of Table I gives the undominated edge profile of quasi-SU 32-cross. In [11], (see also [12]), we demonstrated that SP 32-cross cannot achieve this edge profile by showing that the edge profile for SP-32-cross must have at least eight 1's, rather than the six in the top row of Table I. In [12], we also showed that the largest entry in the SP 32-cross edge profile could not be larger than 10, in contrast to the two 13's in the top row of Table I.

The best SP 32-cross edge profile that we have found through a partial search of the many possible SP labelings is achieved by Fig. 16. Fig. 17 compares the edge profile of the SP 32-cross constellation in Fig. 16 to that of quasi-SU 32-cross. Fig. 17 shows that the quasi-SU 32-cross edge profile dominates the edge profile of this SP 32-cross constellation. The quasi-SU edge profile has a larger value in 12 of the 32 positions, four of which are forced by the restrictions on SP-32-cross discussed above.

The two extra 1's in the SP 32-cross edge profile are inherited by larger SP-cross constellations as well. In general, the standard SP labeling of 2^{2n+1} -cross with $n > 1$ requires $(2n + 4)$ 1's in the edge profile, where quasi-SU labeling only requires $2n + 2$. In this sense, the quasi-SU labeling has a more desirable edge profile.

Despite having more 1's in the edge profile, set partitioning is the clear choice when the encoder trellis has parallel transi-

TABLE I
SIX DISTINCT SQUARED EDGE PROFILE BOUNDS FOR SIX DISTINCT QUASI-GRAY 32-CROSS STRUCTURES

Set 1 (quasi-SU)	1	1	1	1	1	1	2	2	2	2	2	2	2	2	2	4	4	5	5	5	5	5	5	5	5	8	8	8	10	10	13	13
Set 2	1	1	1	1	1	1	2	2	2	2	2	2	2	2	2	4	4	4	5	5	5	5	5	5	5	5	8	8	8	10	13	13
Set 3	1	1	1	1	1	1	2	2	2	2	2	2	2	2	2	4	4	4	5	5	5	5	5	5	5	5	8	8	8	10	13	
Set 4	1	1	1	1	1	1	2	2	2	2	2	2	2	2	2	4	4	4	5	5	5	5	5	5	5	5	5	5	8	8	8	
Set 5	1	1	1	1	1	1	2	2	2	2	2	2	2	2	2	4	5	5	5	5	5	5	5	5	5	8	8	9	10	10	13	
Set 6	1	1	1	1	1	1	2	2	2	2	2	2	2	2	2	4	4	5	5	5	5	5	5	5	5	5	5	8	8	9	10	

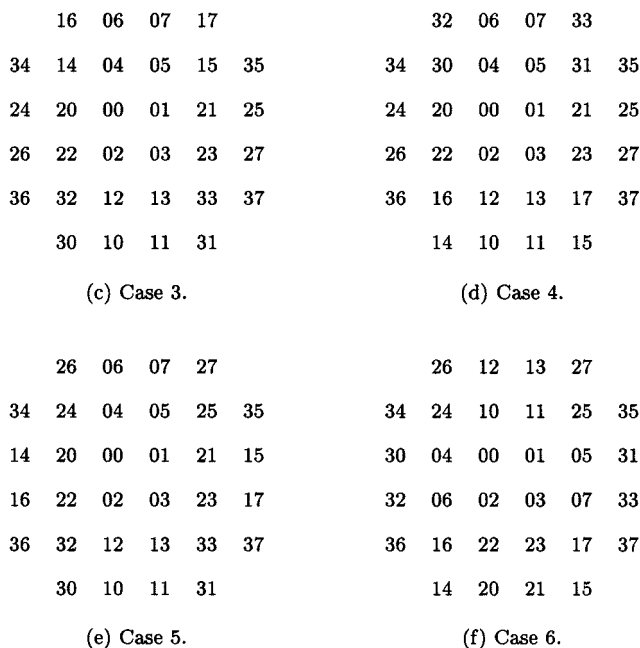
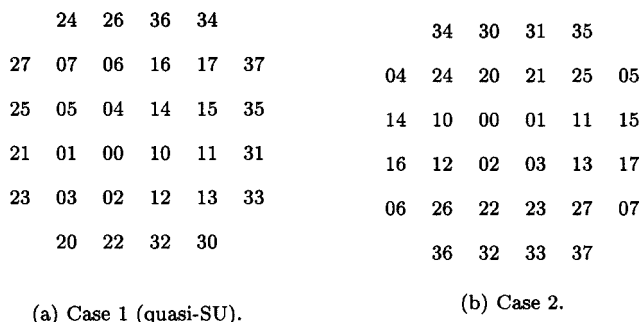


Fig. 15. Constellations labeled in octal according to each of the six distinct quasi-Gray 32-cross labeling structures. Each achieves the edge profile bound for its structure.

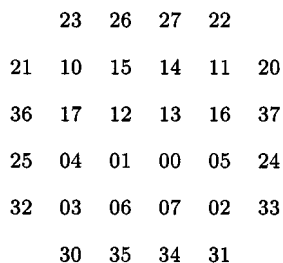


Fig. 16. SP 32-cross used in code searches.

tions. Quasi-SU labeling does not have the proper group structure to protect parallel transitions. Encoders with parallel transi-

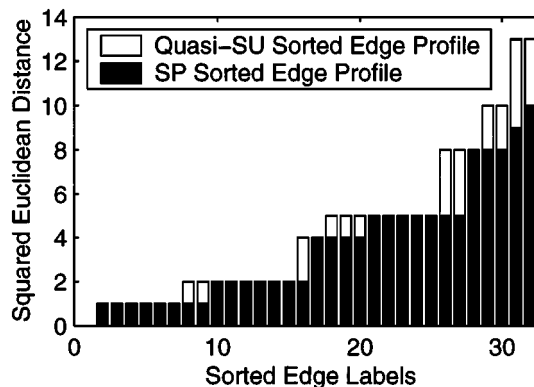


Fig. 17. The sorted edge profiles for quasi-SU 32-cross and the SP 32-cross constellation of Fig. 16. The quasi-SU edge profile dominates the SP edge profile. The two profiles are equal in 20 positions, the quasi-SU profile edge profile is larger in the other 12 positions.

tions are often the optimal choice for practical complexity trellis encoders on the AWGN channel even when the search space is widened to include a trellis without parallel transitions [8].

When the best encoder trellis does not have parallel transitions, then the edge profile becomes the main consideration. Such cases include TCM for fading channels [13] (where the parallel transitions provide no protection from fading), low-rate trellis codes (such as those in [14]), where the relatively small number of trellis branches makes parallel transitions unnecessary, constituent encoders for symbol-interleaved parallel concatenation [15]–[17] (where parallel transitions cause poor decoder performance), and space–time codes [18], [19] (where parallel transitions violate the rank criterion).

In these situations SP labeling is not clearly motivated, and edge-profile-superior labelings can provide an advantage. Simple code design examples illustrate this point. The following example code searches used the quasi-SU 32-cross labeling of Fig. 15(a) and the SP 32-cross labeling of Fig. 16, whose edge profiles are shown in Fig. 17.

As shown in [20], low-rate trellis codes that are robust to severe periodic fading for a specific periodic interleaver can be obtained by maximizing the periodic effective code length (PECL) and the code periodic product distances (CPPDs) with orders ranging from the PECL to the interleaver period. The choice of constellation labeling does not affect the PECL, but it does affect the periodic product distances.

Table II gives an example of a rate-1/5 32-QAM trellis code designed to maximize PECL and the CPPDs for a period-6 interleaver using four memory elements. The largest possible PECL is 5. We seek a code with PECL 5 for which the CPPDs of order 5 and 6 are as large as possible. Table II shows the largest values of the sum of the logs of CPPD₅ and CPPD₆ obtained with each

TABLE II
BEST LOG SUM OF ORDER 5 AND ORDER 6 CPPD WITH FOUR MEMORY ELEMENTS FOR RATE-1/5 32-QAM TRELLIS CODES USING SP AND QUASI-SU 32-CROSS, G_0, G_1, G_2, G_3, G_4 ARE THE GENERATOR POLYNOMIALS OF EACH RATE-1/5 FEEDFORWARD ENCODER

	SP	quasi-SU	Gain
$G_0G_1G_2G_3G_4$	6 7 2 3 27	11 35 37 27 33	
\log_2 CPPD ₅	14.8138	16.0447	1.2317
\log_2 CPPD ₆	11.3219	13.1674	1.8455
Sum	26.1357	29.2122	3.0765

TABLE III
BEST FREE EUCLIDEAN DISTANCES WITH FOUR MEMORY ELEMENTS FOR RATE-1/5 AND RATE-4/5 32-QAM TRELLIS CODES USING SP AND QUASI-SU 32-CROSS

Rate	1/5 ($G_0G_1G_2G_3G_4$)	4/5 ($h_0 h_1 h_2 h_3 h_4$)
SP	36 (06 05 02 22 11)	6 (23 04 16 - -)
quasi-SU	44 (13 17 37 25 23)	4 (21 11 27 23 13)
Gain	0.87 dB	-1.76 dB

of the two labeling paradigms. As expected, the superior edge profile of the quasi-SU 32-cross yields better CPPD values.

In Tables II and III, the generator polynomials of the rate-1/5 feedforward encoders G_0, G_1, G_2, G_3, G_4 are given in octal representation with the least significant bit (LSB) representing the D^0 coefficient of each polynomial. In Table III, the parity polynomials of each canonical systematic feedback rate-4/5 encoder h_0, h_1, h_2, h_3, h_4 are also given in octal representation with the LSB representing the D^0 coefficient of every polynomial. For the mapping of convolutional encoder outputs to constellation points, the LSB of the 32-QAM constellation label is produced by the leftmost polynomial with significance increasing moving left to right.

Table III shows the largest free Euclidean distance obtained by trellis codes with four memory elements at rates 1/5 and 4/5 produced with each of the two labeling paradigms.

Quasi-SU labeling provides 0.87 dB more free Euclidean distance than SP for the rate-1/5 trellis code design. However, quasi-SU labeling provides 1.76 dB *less* Euclidean distance than SP for the rate-4/5 trellis code design. The rate-4/5 largest free Euclidean distance encoder with 32-QAM SP has four parallel branches in each trellis transition.

These code design results support the earlier discussion, i.e., a superior edge profile provides an advantage when the best trellis code does not have parallel transitions, as with the best Euclidean distance rate-1/5 trellis code with four memory elements in Table III. However, traditional SP labeling is, of course, the better choice when the best trellis code does have parallel transitions. This is the case for the best Euclidean distance rate-4/5 trellis code with four memory elements in Table III.

Perhaps even high-rate trellis codes benefit from a superior edge profile when the number of trellis states is large enough that the best trellis code does not employ parallel transitions.

V. CONCLUSION

This paper examined constellation labelings in the context of their edge profile, the list of minimum-distance edges for each binary symbol error. Neither GC labeling nor set-partitioning uniquely specifies the labeling structure. There remains some

freedom to choose the final labeling within either paradigm, and this choice can affect trellis code performance. For 2^n -PSK or PAM and 2^{2n} -point square QAM, the class of SU labelings (a generalization of the commonly used reflected binary GC) provides undominated edge profiles. SU labelings can produce the standard set-partitioning and GC labelings for these constellations.

2^{2n+1} -point cross constellations must have at least $2n+2$ distinct labels for the minimum-distance edges, i.e., GC labeling is impossible for cross constellations. This paper gives a simple procedure for producing quasi-Gray labelings having exactly $2n+2$ distinct labels for the minimum-distance edges. In contrast, set partitioning of 2^{2n+1} -cross requires $2n+4$ minimum-distance edge labels.

Thus, for cross constellations there is a choice between edge profile optimality and the group structure provided by set partitioning. In a low-complexity code search example, set partitioning is superior when there are parallel trellis branches in the best encoder but edge-profile optimality is better when the best encoder does not have parallel trellis branches.

Quasi-SU should be the proper labeling strategy for cross constellations whenever parallel branches must be avoided. Some example applications include trellis codes for fading channels [13], trellis codes that protect against periodic erasures [14], space-time codes [18], [19], and symbol-interleaved turbo codes [15]–[17]. Generally, the results of this paper apply directly to linear encoders that map binary symbols to one of the standard 2-D constellations.

Care must be taken when applying our results to bit-interleaved coded modulation (BICM) with or without concatenation and iterative decoding. With BICM, performance depends on both the Euclidean distance and the value of the edge label itself [21], [22]. The most important condition for BICM with the single iteration decoding of [21], [22] is that all (for cross constellations, almost all) of the difference labels have unit Hamming weight. SU or quasi-SU labelings with difference labels chosen to meet the Gray or quasi-Gray condition should also be the best choice for BICM in this case.

When multiple iterations are employed at the decoder, as described in [23], [24], the best choice of labeling depends on the number of iterations used. The more iterations used, the less the labeling looks like a Gray labeling. Perhaps all the best labelings here are SU or quasi-SU, and what changes is the choice of basis. The questions raised in [23], [24] make labeling for the BICM systems an interesting area for future investigation.

There are several other open questions available for further research. While we showed that SU labeling provides an undominated edge profile, we did not show that SU edge profiles dominate all others. From [8], the SU edge profile dominates all others for 8-PSK and 16-QAM. Theorem 3 restricts potential labelings with edge profiles undominated by the SU edge profile to be nonultracomposite. However, whether SU edge profiles generally dominate all others remains an open question. For cross constellations, we did not even show that quasi-SU edge profiles are always undominated. This is true for 32-cross, and it might be true in general.

Another interesting area is the relationship between the trellis and the choice of labeling structure. For cross constellations,

one might also explore how the group constraints imposed to maintain an edge profile and by set partitioning might be combined. For a trellis with relatively few parallel branches, one could impose group constraints less comprehensive than a full set partitioning in return for an improved edge profile. This might yield a better labeling structure for the particular trellis, one that lies between the extremes of SP and quasi-SU.

Finally, this paper focused on the standard PAM, PSK, square-QAM, and cross constellations. Future work should address both the design of new nonstandard constellations and the associated labeling of such constellations. Fragouli *et al.* in [25] provide an example of the possibilities.

APPENDIX A EXAMPLE OF THEOREM 1 RECURSION

The proofs of Lemmas 1–4 and Theorem 1 all follow the basic principle of determining the structural constraints required to at least achieve each position of the SU edge profile. This is accomplished by working from the edges of the sorted edge profile toward the center.

For this approach to work, the progression toward the center cannot skip any values. For example, it is not useful to limit the number of 3's in the edge profile to be less than or equal to that of the SU profile without first limiting the number of 1's and 2's. Otherwise, the number of 3's might be trivially kept small at the cost of a large number of 1's. Having edge labels of distance-3 edges also appear on distance-1 edges would accomplish this. The resulting edge profile would have fewer 3's than the SU edge profile but more 1's, producing an edge profile that cannot dominate the SU profile.

The purpose of this appendix is to show that no values in the edge profile are skipped in the recursive application of Lemmas 1–4 in the proof of Theorem 1. It would appear at first that some values are indeed skipped. However, the additional structure in the labeling imposed with each recursion is exactly enough to show that no values are skipped after all.

Consider how Theorem 1 applies to 32-PAM. The first application of the four lemmas guarantees that

$$\langle P \rangle = [1 \ 1 \ 1 \ 1 \ 1 \ 2 \ 2 \ 2 \ 2 \ \dots \ 15 \ 16]$$

and forces the structure of either (14) or (15) on the difference list. Noting the structure forced by Lemma 2, (14) and (15) show only the first half of the difference list

$$L = \begin{bmatrix} b_1 & e_2 & b_1 & e_4 & b_1 & e_6 & b_1 & e_8 & \dots \\ b_1 & e_{10} & b_1 & e_{12} & b_1 & e_{14} & b_1 & e_{16} & \dots \end{bmatrix} \quad (14)$$

$$L = \begin{bmatrix} e_1 & b_1 & e_3 & b_1 & e_5 & b_1 & e_7 & b_1 & \dots \\ e_9 & b_1 & e_{11} & b_1 & e_{13} & b_1 & e_{15} & b_1 & \dots \end{bmatrix}. \quad (15)$$

For each of these two difference lists, we apply Lemmas 1–4 to a 16-PAM subconstellation obtained by taking every other point in the original 32-PAM constellation. We still assume unit distance between neighboring points. Hence, a distance of 1 between neighbors in the newly constructed 16-PAM constellation corresponds to a distance of 2 in the original 32-PAM constellation.

Lemmas 1–4 applied to this constellation force the 16-PAM edge profile to have exactly four 1's, exactly one 8, exactly three 2's, and exactly one 7, respectively. These constraints corre-

spond to forcing the original 32-PAM edge profile to have exactly four 2's, exactly one 16, exactly three 4's, and exactly one 14, respectively. It would appear that this second application of Lemmas 1–4 has skipped the value of 3 in the 32-PAM edge profile.

However, the structure of (14) and (15) actually forces the number of 3's to be exactly the same as the number of 4's. Note that an edge label for a distance-3 edge has two possible structures: either $b_1 \oplus e_i \oplus b_1$ or $e_i \oplus b_1 \oplus e_j$. Furthermore, $b_1 \oplus e_i \oplus b_1 = e_i$ so that this edge label has minimum distance 1. Thus, only labels with the structure $e_i \oplus b_1 \oplus e_j$ have minimum distance 3.

For each distance-3 edge with such a label, there is a distance-4 edge labeled

$$b_1 \oplus e_i \oplus b_1 \oplus e_j = e_i \oplus e_j \quad (16)$$

obtained by adding an additional b_1 to one of the two ends. Similarly, for every distance-4 edge there is a distance-3 edge obtained by removing the b_1 from the end. Thus, the number of 3's in the edge profile is exactly the same as the number of 4's in the edge profile. For this structure, restricting the number of 4's in the edge profile is equivalent to simultaneously limiting the number of 3's and 4's.

In fact, this argument easily generalizes to show that with a constellation where every other difference label is set to b_1 , for each odd number $k > 1$, the number of k 's in an edge profile must be the same as the number of $(k+1)$'s. Thus, by forcing exactly one 14 in the edge profile, we have also forced exactly one 13 in the edge profile.

The 16-PAM subconstellation has difference labels of the form $b_1 \oplus e_i$. Thus, forcing every other difference label of the 16-PAM subconstellation to be identical (using Lemma 4) forces every other unassigned difference label (i.e., labels other than b_1) in our original 32-PAM to be identical. Using our ordered introduction of basis labels, we assign these difference labels to be b_2 .

Starting from (14), the two possibilities are

$$L = \begin{bmatrix} b_1 & b_2 & b_1 & e_4 & b_1 & b_2 & b_1 & e_8 & \dots \\ b_1 & b_2 & b_1 & e_{12} & b_1 & b_2 & b_1 & e_{16} & \dots \end{bmatrix} \quad (17)$$

$$L = \begin{bmatrix} b_1 & e_2 & b_1 & b_2 & b_1 & e_6 & b_1 & b_2 & \dots \\ b_1 & e_{10} & b_1 & b_2 & b_1 & e_{14} & b_1 & b_2 & \dots \end{bmatrix}. \quad (18)$$

Starting from (15), the two possibilities are

$$L = \begin{bmatrix} b_2 & b_1 & e_3 & b_1 & b_2 & b_1 & e_7 & b_1 & \dots \\ b_2 & b_1 & e_{11} & b_1 & b_2 & b_1 & e_{15} & b_1 & \dots \end{bmatrix} \quad (19)$$

$$L = \begin{bmatrix} e_1 & b_1 & b_2 & b_1 & e_5 & b_1 & b_2 & b_1 & \dots \\ e_9 & b_1 & b_2 & b_1 & e_{13} & b_1 & b_2 & b_1 & \dots \end{bmatrix}. \quad (20)$$

With the additional structure provided by b_2 , arguments similar to those above place even more structure on the edge profile. If there is an edge of length k with leftmost difference label e_i and rightmost difference label e_j , with $e_i \neq e_j$, and $e_i, e_j \notin \{b_1, b_2\}$, then the edge profile will have the same number of k 's, $(k+1)$'s, $(k+2)$'s, and $(k+3)$'s. An example of this is the edge of length $k = 5$ with label $e_1 \oplus b_1 \oplus b_2 \oplus b_1 \oplus e_5$ in (20) above.

Edge labels with an e_i and an e_j at the ends are the only ones that have minimum distance k , and each of these has corresponding edge labels with minimum distances $k+1$, $k+2$, and $k+3$ as b_1 , $b_1 \oplus b_2$, and $b_1 \oplus b_2 \oplus b_1$ are added to the end.

For each of the four difference lists (17)–(20) we apply Lemmas 1–4 to an 8-PAM subconstellation obtained by taking every fourth point in the original 32-PAM constellation. These 8-PAM subconstellations have difference labels of the form $b_2 \oplus e_i$. Lemmas 1–4 applied to this constellation force the 8-PAM edge profile to have exactly three 1’s, exactly one 4, exactly two 2’s, and exactly one 3, respectively. These constraints correspond to exactly three 4’s, exactly one 16, exactly two 8’s, and exactly one 12 in the edge profile of the original 32-PAM constellation.

Here again, one might consider it premature to force exactly two 8’s when the number of 5’s, 6’s, and 7’s have not been specifically constrained. However, as discussed above, the structure imposed by the placement of b_1 ’s and b_2 ’s means that the number of 5’s, 6’s, 7’s, and 8’s in the edge profile will be the same. Also note that forcing exactly one 16 also forces exactly one 13, one 14, and one 15. At this point, the entire edge profile has been forced to be exactly the SU edge profile.

Applying Lemmas 1–4 to (17)–(20) by labeling every other unassigned position with b_3 produces eight difference lists each with exactly four difference labels yet to be assigned a basis label. However, for each of these difference lists, the four unassigned difference labels consist of two instances each of two distinct difference labels, say e_i and e_j . At this point, any matching of b_4 and b_5 to e_i and e_j produces an equivalent structure.

Furthermore, examining these difference lists reveals that each one achieves exactly the edge profile of SU 32-PAM. Actually, the only additional observation required for this is that the number of 12’s in the edge profile also determines the number of 9’s, 10’s, and 11’s. Note that some of these difference lists are exactly SU 32-PAM, but some are shifted versions of the SU labeling, and as such are not even ultracomposite.

In general, at the i th level of the recursion, the placement of b_1, \dots, b_i forces groups of 2^i distances to have the same multiplicity in the edge profile. The smallest distance in each such group corresponds to an edge with an e_i and an e_j at the ends. That is, the difference labels at the ends are not labeled with any of the assigned basis vectors b_1, \dots, b_i .

This grouping of multiplicities is just sufficient to permit the application of Lemmas 1–4 at the next level of recursion to place constraints on the edge profile that continue working from the edges toward the center without skipping any values. For a 2^n -PAM constellation, $n-2$ levels of recursion completely constrain the edge profile to be exactly the SU edge profile.

APPENDIX B
8-QAM LABELING

This appendix considers labeling for the standard 8-QAM constellation shown in Fig. 18. While considered one of the cross constellations, this constellation does not have the central-square-with-four-wings structure of all the other cross constellations, and this structural distinction leads to a different labeling behavior than what was shown in Section IV. The procedure outlined in Theorem 5 does not apply to 8-QAM.

In contrast to the larger cross constellations, we show below that all standard SP-labeled 8-QAM constellations achieve the best possible edge profile. This structure can be either SP

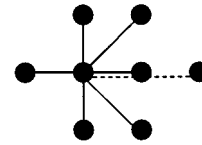


Fig. 18. Edges for profile upper bound of 8-QAM.

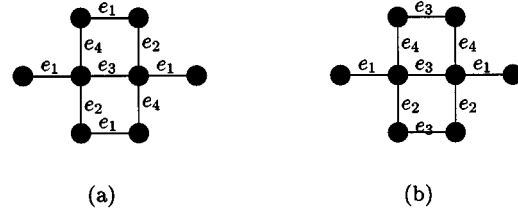


Fig. 19. The two labeling structures achieving the superior edge profile for 8-QAM constellations.

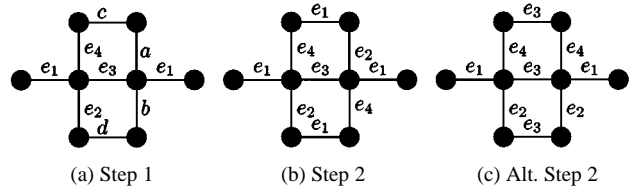


Fig. 20. Steps to achieve SP labeling of 8-QAM.

or quasi-Gray depending on the choice of basis. In this way, 8-QAM is similar to PSK and square QAM where a single optimal labeling structure supports either SP or GC.

Fig. 18 shows the edges emanating from one of the two central points in an 8-QAM constellation (tilted 45° for simplicity). These edges provide an upper bound on the achievable edge profile for 8-QAM

$$\langle P^2(8\text{-QAM}) \rangle \leq [0 \ 1 \ 1 \ 1 \ 1 \ 2 \ 2 \ 4]. \quad (21)$$

Fig. 19 illustrates the two distinct quasi-Gray labeling structures for 8-QAM that also achieve the edge profile bound of (21). There are other quasi-Gray labelings of 8-QAM that do not achieve the edge profile of (21) [10]. In Fig. 19(a), $e_4 = e_1 \oplus e_2 \oplus e_3$ since these four edges form a cycle. In Fig. 19(b), the possibilities for e_4 are $e_4 = e_1 \oplus e_2$ or $e_4 = e_1 \oplus e_2 \oplus e_3$ since $e_4 \oplus e_1 \oplus e_3$ and $e_4 \oplus e_2 \oplus e_3$ label paths that are not cycles.

Theorem 6: All SP labelings of 8-QAM achieve the edge profile bound of (21).

Proof: First note that any SP labeling of 8-QAM causes unit-distance horizontal edge labels to alternate between exactly two different 3-bit labels, which differ only in the third (the most significant) bit. Vertical unit-distance edge labels alternate between a different pair of labels. Altogether, the vertical and horizontal unit-distance edge labels consist of four distinct labels, which are selected from $\{001, 011, 101, 111\}$. Each of these unit-distance edge labels is the sum of the other three unit-distance edge labels. These restrictions make an enumeration of SP labeling structures for 8-QAM straightforward.

Fig. 20(a) begins this enumeration by using the four distinct edge labels to label the four edges emanating from one of the two central points. The alternating label rule also forces placement of an additional e_1 label. Fig. 20(b) and (c) shows the only

two ways to complete the SP labeling while obeying the alternation rule. These two labeling structures are exactly the two structures identified in Fig. 19 as achieving (21).

ACKNOWLEDGMENT

The authors wish to thank the anonymous reviewers for their comments, which greatly improved the paper. The authors thank B. Ryan, S. Benjamin, and A. Bernard for carefully reading several versions of the manuscript and providing many helpful comments. Finally, the authors thank P. Örmeci and D. Goeckel for inspiring the general procedure for quasi-Gray labeling cross constellations.

REFERENCES

- [1] F. Gray, "Pulse code communications," U.S. Patent 2 632 058, Mar. 1953.
- [2] G. Ungerboeck, "Channel coding with multilevel/phase signals," *IEEE Trans. Inform. Theory*, vol. IT-28, pp. 55–67, Jan. 1982.
- [3] ———, "Trellis-coded modulation with redundant signal sets—Parts I and II," *IEEE Commun. Mag.*, vol. 25, pp. 5–20, Feb. 1987.
- [4] G. D. Forney, Jr., "Convolutional codes I: Algebraic structure," *IEEE Trans. Inform. Theory*, vol. IT-16, pp. 720–738, Nov. 1970.
- [5] R. D. Wesel, "Reduced complexity trellis code transfer function computation," in *Proc. Communication Theory Mini-Conf. at IEEE Int. Conf. Communications*, Vancouver, B.C., Canada, June 1999, pp. 37–41.
- [6] S. G. Wilson and Y. S. Leung, "Trellis coded phase modulation on Rayleigh channels," in *Proc. IEEE Int. Conf. Communications*, Seattle, WA, June 1987, pp. 739–743.
- [7] D. Divsalar and M. K. Simon, "The design of trellis coded MPSK for fading channels: Performance criteria," *IEEE Trans. Commun.*, vol. 36, pp. 1004–1012, Sept. 1988.
- [8] R. D. Wesel, "Trellis code design for correlated fading and achievable rates for Tomlinson–Harashima precoding," Ph.D. dissertation, Stanford Univ., Stanford, CA, Aug. 1996.
- [9] E. N. Gilbert, "Gray codes and paths on the n -cube," *Bell Syst. Tech. J.*, vol. 37, pp. 815–826, May 1958.
- [10] X. Liu and R. D. Wesel, "Profile optimal 8-QAM and 32-QAM constellations," in *Proc. 36th Annu. Allerton Conf. Communication, Control, and Computing*, Monticello, IL, Sept. 1998, pp. 136–145.
- [11] X. Liu, "Trellis code design for periodic erasures and adaptive coded modulation schemes for time-varying channels," Ph.D. dissertation, Univ. Calif., Los Angeles, Dec. 2000.
- [12] R. D. Wesel, C. Komninakis, and X. Liu, "Toward optimality in constellation labeling," in *Proc. Communication Theory Mini-Conf. at IEEE Global Telecommunications Conf.*, Phoenix, AZ, Nov. 1997, pp. 23–27.
- [13] J. Du, Y. Kamio, H. Sasaoka, and B. Vucetic, "New 32-QAM trellis codes for fading channels," *Electron. Lett.*, vol. 29, no. 20, pp. 1745–1746, Sept. 1993.
- [14] R. D. Wesel, X. Liu, and W. Shi, "Trellis codes for periodic erasures," *IEEE Trans. Commun.*, vol. 48, pp. 938–947, June 2000.
- [15] P. Robertson and T. Worz, "Bandwidth-efficient turbo trellis-coded modulation using punctured component codes," *IEEE J. Select. Areas Commun.*, vol. 16, pp. 206–218, Feb. 1998.
- [16] C. Fragouli and R. D. Wesel, "Symbol-interleaved parallel concatenated trellis coded modulation," in *Proc. Communication Theory Mini-Conf. at IEEE Int. Conf. Communications*, Vancouver, B.C., Canada, June 1999, pp. 42–46.
- [17] ———, "Turbo encoder design for symbol-interleaved parallel concatenated trellis coded modulation," *IEEE Trans. Commun.*, vol. 49, pp. 425–435, Mar. 2001.
- [18] J.-C. Guey, M. P. Fitz, M. R. Bell, and W.-Y. Kuo, "Signal design for transmitter diversity wireless communication systems over Rayleigh fading channels," *IEEE Trans. Commun.*, vol. 47, pp. 527–537, Apr. 1999.
- [19] V. Tarokh, N. Seshadri, and A. R. Calderbank, "Space-time codes for high data rate wireless communication: Performance criterion and code construction," *IEEE Trans. Inform. Theory*, vol. 44, pp. 744–765, Mar. 1998.
- [20] R. D. Wesel and J. M. Cioffi, "Trellis code design for periodic interleavers," *IEEE Commun. Lett.*, vol. 3, pp. 103–105, Apr. 1999.
- [21] E. Zehavi, "8-PSK trellis codes for a Rayleigh fading channel," *IEEE Trans. Commun.*, pp. 873–884, May 1992.
- [22] G. Caire, G. Taricco, and E. Biglieri, "Bit interleaved coded modulation," *IEEE Trans. Inform. Theory*, vol. 44, pp. 927–946, May 1998.
- [23] S. ten Brink, J. Speidel, and R.-H. Yan, "Iterative demapping and decoding for multilevel modulation," in *Proc. IEEE Global Telecommunications Conf.*, Sydney, NSW, Australia, Nov. 1998, pp. 579–584.
- [24] ———, "Iterative demapping and decoding for QPSK modulation," *Electron. Lett.*, vol. 34, no. 15, pp. 1459–1460, July 1998.
- [25] C. Fragouli, R. D. Wesel, D. Sommer, and G. Fettweis, "Turbo codes with non-uniform QUAM constellations," in *Proc. Int. Conf. Communications (ICC) 2001*, Helsinki, Finland, June 11–14, 2001, pp. 70–73.